

Studies on Microstructure and Mechanical Properties of Simulated Heat Affected Zone in a Micro Alloyed Steel

Sanjeev Kumar, S. K. Nath

Abstract—Proper selection of welding parameters for getting excellent weld is a challenge. HAZ simulation helps in identifying suitable welding parameters like heating rate, cooling rate, peak temperature, and energy input. In this study, the influence of weld thermal cycle of heat affected zone (HAZ) is simulated for Submerged Arc Welding (SAW) using Gleeble® 3800 thermo-mechanical simulator. A (Micro-alloyed) MA steel plate of thickness 18 mm having yield strength 450MPa is used for making test specimens. Determination of the mechanical properties of weld simulated specimens including Charpy V-notch toughness and hardness is performed. Peak temperatures of 1300°C, 1150°C, 1000°C, 900°C, 800°C, heat energy input of 22KJ/cm and preheat temperatures of 30°C have been used with Rykalin-3D simulation model. It is found that the impact toughness (75J) is the best for the simulated HAZ specimen at the peak temperature 900°C. For parent steel, impact toughness value is 26.8J at -50°C in transverse direction.

Keyword—HAZ Simulation, Mechanical Properties, Peak Temperature, Ship hull steel, and Weldability.

I. INTRODUCTION

MICRO alloyed (MA) steels have witnessed rapid growth because of the great progress of modern metallurgical technology in recent years. These steels have become one of the most dynamic steels in the world. MA steels having less than 5% alloys provide better mechanical properties than carbon steel. It is being increasingly used in large scale into the shipbuilding industry. Different types of welding techniques like as Gas metal arc welding, metal inert gas arc welding, and Submerged arc welding are being used [1]. There are two types of problems that occur at time of welding by fusion welding processes, one is the cold crack by quenched structure and another weld joints having always higher impact strength than the parent metal [2]. Rapid heating and cooling with negligible hold time at peak temperature usually characterizes the weld thermal cycle in thick plates [3]. X. U. W. W. et al [4] have studied effect of correlation between heat inputs, microstructure and impact toughness of the HAZ using Gleeble simulation technique. They have found higher impact

energy if heat input less than 22kJ while the heat input higher than 40kJ, lower impact energy is noted. It has been attributed to the increase of the amount of grain boundary ferrite (GBF). The ratio of lath martensite to retained austenite (M-A) and average size of micro-constituent increased with increasing heat input. M. Shome et al [5] have worked on two different heat input single cycle with two types of HSLA steel. They have observed the prior-austenite grain size is grow rapidly beyond 1100°C in both the steels, primarily with the dissolution of niobium carbonitride precipitates. A. Ghosh et al have studied an ultra-low carbon HSLA steel. This steel was subjected to two stages forging with different post cooling techniques. They have found better strength at faster cooling rate due to its highly dislocated acicular ferrite structure along with fine precipitation of carbides and carbonitrides. However, ductility decreases. But at the slower cooling rate both properties are reversed. Mechanical properties of materials into heat affected zone have depended upon the heating and cooling rate of thermal cycle [6], [7]. Fatih Hayat et al. [8] have worked on the effect of heat treatment on mechanical properties and fracture behaviour of grade A in 4 different composition and dual phase steels. They have found in this work specimens of grade A and dual phase steel had quenched at 800°C and 900°C better strength than DH36 steel. Tensile strength of dual phase steel at 900°C water quenched was better than 3 and 2 times of grade A and DH36 steel respectively.

The objective of this work is to assess the weldability of HSLA steel with help of HAZ simulation by Thermo mechanical simulator (TMS), Gleeble 3800. These simulations help in generating optimum welding parameters for shipbuilders.

II. MATERIALS AND METHOD

A. Material

The chemical composition of steel used is given in Table I. The test material was received from the UP government workshop, Roorkee, Uttarakhand. It is a 450 MPa grade micro alloy steel of 18 mm thickness.

TABLE I
CHEMICAL COMPOSITION OF MA STEEL (WT %)

C	Si	Mn	P	S	Al	Nb	V
0.14	0.25	1.52	0.03	0.007	0.02	0.04	0.01

Sanjeev Kumar is research scholar in Metallurgical and Materials Engineering Department, Indian Institute of Technology Roorkee, Uttarakhand, India (e-mail: rajputskmt@gmail.com).

S. K. Nath is Professor & Head in Metallurgical and Materials Engineering Department, Indian Institute of Technology Roorkee, Uttarakhand, India (e-mail: indiafmt@iitr.ernet.in).

B. Dilatometry Test Method

The sample used in the dilatometer test is a cylindrical rod 10 mm in diameter and 70 mm in length. To measure the critical temperature of steel samples were at first austenitized at the rate of 200°C/s upto 1350°C and held for 0.1sec, and then cooled to room temperature at the rate of 10°C/s. Dimensional change in the specimen were measured by the dilatometer in TMS.

C. HAZ Simulation Method

The HAZ simulation was conducted in TMS. Fig. 1 shows specimen (10mm×10mm×70mm) for the thermal cycle. HAZ simulation thermal cycles corresponding to Rykalin-3D (thick plate) formulation [9], which is based on conductive heat transfer is used. A chromel-Alumel thermocouple was welded at the centre of the specimen.

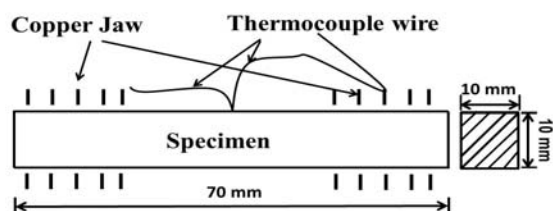


Fig. 1 Typical HAZ thermal profile of a HAZ simulation at different peak temperatures

Fig. 2 shows single thermal cycle simulation were done with different peak temperatures (T_p) but a fixed cooling rate $\Delta t_{8/5}$, which represents the time required to cool from 800°C to 500°C. The specimens were uniformly heated at 200°C/s and after heating the specimen was held for a very short duration of time (0.1 seconds) and then cooled.

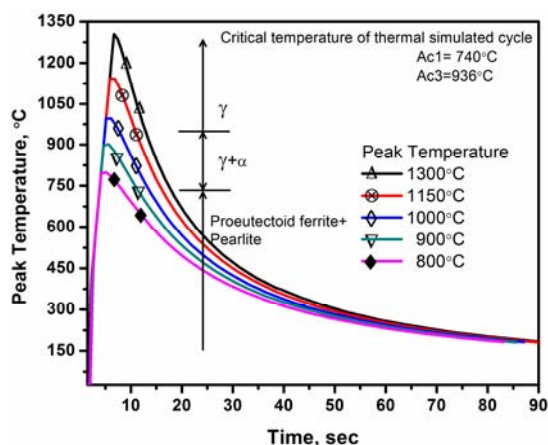


Fig. 2 Typical HAZ thermal profile of a HAZ simulation at different peak temperatures

The peak temperature, heat input, preheat temperature and cooling rate of the HAZ thermal cycle parameters were selected according to possible submerged arc welding (SAW). After the HAZ simulation, the simulated specimens were made V-notch where thermo couple welds at the time HAZ simulation.

Table II shows cooling rate and heating time interval for various peak temperatures have been found in the thermal cycle.

TABLE II
 TIME INTERVALS OF THERMAL CYCLING PARAMETERS FOR DIFFERENT PEAK TEMPERATURES

Peak Temperature (T_p) °C	Heating time (s) from room Temperature to T_p	Cooling time (s) from Peak Temperature to 800°C	Cooling time (s) from 800°C to 500°C	Cooling Rate °C /s $\Delta t_{8/5}$
1300	6.35	9.4	11.9	25.2
1150	5.6	8.5	11.9	25.0
1000	4.85	5.4	12.6	23.8
900	4.35	3.7	12.7	23.7
800	3.85	---	14.3	21.0

D. Mechanical Testing & Characterization Method

Test samples for Charpy V-notch (CVN) impact toughness evaluation were prepared according to the ASTM E 23 [10] standard. After the HAZ simulation, V-notch was made where thermocouple was welded. Charpy test have been done for impact properties in cryogenic temperature -50°C of as-received and simulated samples. After the charpy test, one part was used for metallographical examination and hardness measurement; other part was used for factography.

The samples for hardness measurement were prepared according to the ASTM E92-82 [11] standard. The as-received and HAZ simulated samples of MA steel specimen were prepared for metallographic examination. Samples were etched using Nital reagent (2 ml nitric acid, and 98 ml methanol). A Leica DMI 5000M optical microscope equipped with digital imaging facility was used to record the microstructures. SEM fractographs were taken in Zeiss EVO 18 scanning electron microscope.

III. RESULTS AND DISCUSSION

A. Dilatometry

Fig. 3 shows the plot between dialation and temperature. It can be observed that during heating there is change in slope corresponding to lower critical temperature (A_1) which is found to be 740°C and further heating of the sample results again in change of slope corresponding to upper critical temperature (A_3) is 936°C. It is observed that there is increase in length as the sample is heated due to thermal expansion.

The change in slope at lower critical temperature is attributed to formation of closed pack structure (austenite) from BCC α -iron of the steel. The change in slope at upper critical temperature is again attributed to completely transforming the steel into closed packed γ (austenite) from ($\alpha+\gamma$) region. Further increase in temperature causes expansion in the sample due to thermal expansion.

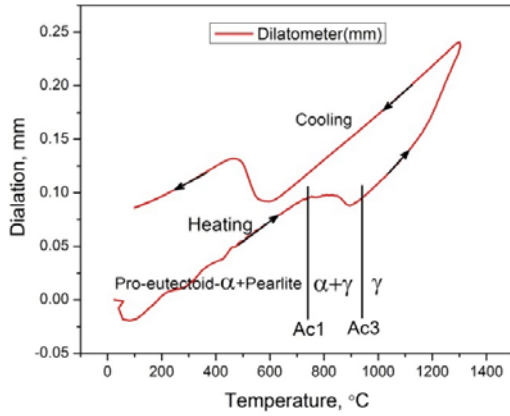


Fig. 3 Dialatoin curve for MA steel

B. Microstructure

Figs. 4 (a)-(f) show optical micrographs of as-received and various HAZ simulated specimens. As received specimen shows proeutectoid ferrite (white region) and pearlite (black region), Fig. 4 (a) Pearlite is appearing in banded form. This banded structure is typical of thick steel plates. Fig. 4 (b) is also proeutectoid ferrite and pearlite. However, here pearlite has been refined as peak temperature in HAZ has reached in the intercritical (A_1 - A_3) temperature zone. Figs. 4 (c), (d) show lots of refinement in proeutectoid ferrite and pearlite as peak temperature is in single phase austenite region of Fe-C phase diagram. Fig. 4 (e) shows acicular ferrite and pearlite and some amount of bainite. Fig. 4 (f) shows grain coarsening in the prior austenite grain size. Martensite is visible within the austenite grains.

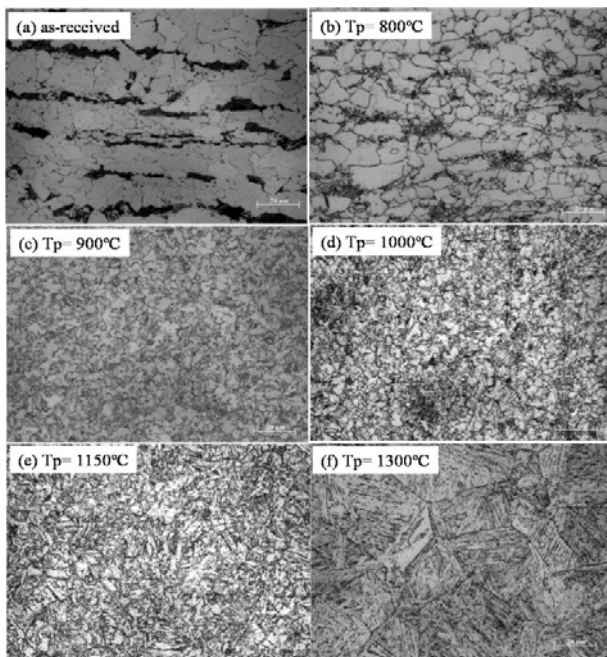


Fig. 4 Optical micrographs of as-received and HAZ simulated samples at different peak temperatures

C. Mechanical Properties

The variation of hardness with peak temperature is shown in Fig. 5 with increase in peak temperature hardness increases. This has been attributed to refinement in the structure and formation of acicular structure. The maximum hardness is observed where fully martensitic structure is observed (Fig. 4 (f)).

The variation of impact toughness with peak temperature is shown in Fig. 6. All the impact toughness is measured at -50°C . As-received specimen has impact toughness value of 26.82J. It is observed that impact toughness first increases and then decreases. A Maximum value of impact toughness 75J has been observed for peak temperature 900°C . This peak in impact toughness is due to formation of fine grained structure. The lowest value in impact toughness (16.5J) is attributed to grain coarsening and formation of fully martensitic structure.

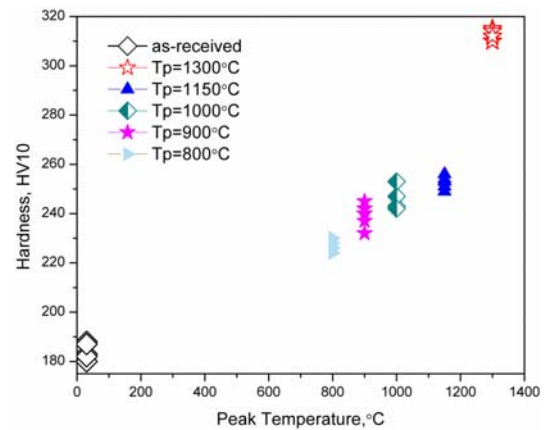


Fig. 5 Hardness of HAZ subjected to thermal cycles with different peak temperatures

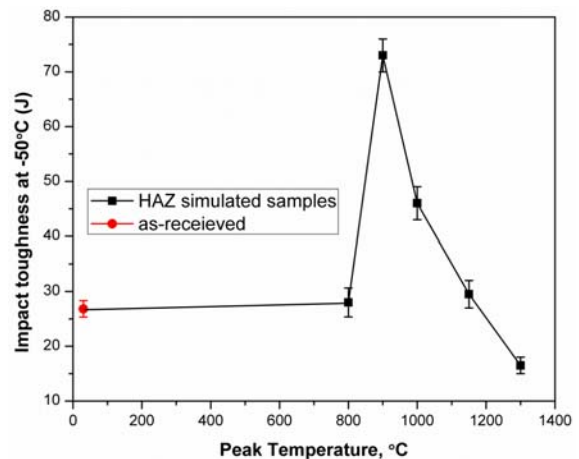


Fig. 6 Impact properties of HSLA steel at different peak temperatures tested at -50°C

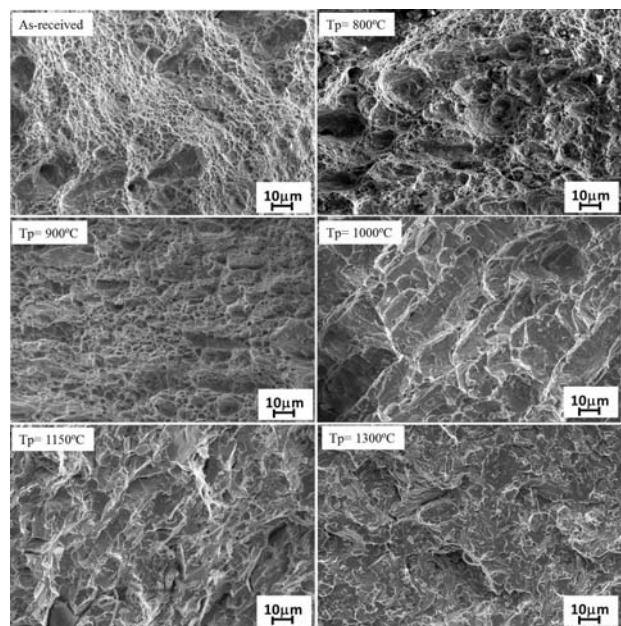


Fig. 7 SEM micrographs of as-received and HAZ simulated samples at different peak temperatures

All the SEM fractographs of broken impact test specimens exhibit brittle fracture mode as all impact tests have been performed at -50°C (Fig. 7). It is consistent with results of researchers [12].

IV. CONCLUSIONS

Following conclusions can be drawn from the present investigation:

1. Microstructural refinement was seen in all simulated samples as compared to the as-received MA steel sample except for sample attaining peak temperature 1300°C .
2. Hardness values of all HAZ simulated samples increased with peak temperature as compared to as-received steel.
3. As compared to as-received steel, the impact energy values increased upto peak temperature 900°C and decreased consistently with increase in peak temperature. The highest and lowest impact energy values were observed for peak temperatures of 900°C and 1300°C respectively.
4. A Maximum value of impact toughness 75J has been observed at 900°C due to formation of fine grained structure. As-received specimen has value of 26.82 J.
5. In present study best combination of mechanical properties and microstructural refinement are obtained for the steel simulated at the peak temperature 900°C .

ACKNOWLEDGEMENT

Authors are grateful to DST New Delhi for the FIST grant to acquire Thermo Mechanical Simulator.

REFERENCES

- [1] R Datta, D Mukerjee, K L Rohira, R Veeraraghavan, "Weldability evaluation of high tensile plates using GMAW process", *Journal of Materials Engineering Performance*, 8(4), 55-62, 1999.
- [2] P Yayla, E Kaluc, K.Ural, "Effects of welding processes on the mechanical properties of HY 80 steel weldments", *Materials and Design* 28(1), 898-906, 2007.
- [3] W.W Xu, Q. E Wang, T. Pan, H. Su, and C.E Yang, "Effect of Welding Heat Input on Simulated HAZ Microstructure and Toughness of a V-N Microalloyed Steel", *Proceedings of Sino-Swedish Structural Materials Symposium*, 234-239, 2007.
- [4] A Ghosh, S. Das, S. Chatterjee, and P. Ramachandra Rao, "Effect of cooling rate on structure and properties of an ultra-low carbon HSLA-100 grade steel", *Materials Characterization*, 56, 59-65, 2006.
- [5] M. Shome, O.P. Gupta, and O.N. Mohanty, "Effect of Simulated Thermal Cycles on the Microstructure of the Heat-Affected Zone in HSLA-80 and HSLA-100 Steel Plates", *Metallurgical and Materials Transactions A*, 35A, 985-996, 2004.
- [6] L.E. Svensson, "Control of Microstructures and Properties in Steel Arc Welds", *CRC Press, Boca Raton, FL*, 101-106, 1994.
- [7] D. Radaj, "Heat Effects of Welding, Springer-Verlag Publications, Heidelberg", 100-103, 1992.
- [8] Fatih Hayat, Huseyin Uzun, "Effect of Heat Treatment on Microstructure Mechanical Properties and Fracture Behaviour of Ship and Dual Phase Steels", *Journal of iron and steel Research, International*. 18(8), 65-72, 2011.
- [9] N.N. Rykalin, "Calculation of Heat Flow in Welding Document", *International Institute of Welding London*, 212-350, 1974.
- [10] ASTM E 23 standard test methods for notched bar impact testing of metallic materials.
- [11] ASTM E92-82 standard test methods for vickers hardness of metallic materials.
- [12] Ernest C. Rollason, "Metallurgy for engineers", 1961.